Hybrid Position/Force Control of Flexible Manipulators

°Jin-Soo Kim* Kuniaki Suzuki * Atsushi Konno ** Masaru Uchiyama*

*Department of Aeronautics and Space Engineering, Tohoku University Aoba-ku, Sendai 980-77, Japan

Tel: +81 22 217-6973; FAX : +81 22 217-6971; E-mail: kim@space.mech.tohoku.ac.jp

** Department of Mechano-Informatics, University of Tokyo Bunkyo-ku, 113 Tokyo, Japan

Tel: +81 3 3812-2111 Ext.7415; FAX: +81 3 3815-8356; E-mail: konno@jsk.t.u-tokyo.ac.jp

Abstract In this paper, we discuss the force control of flexible manipulators. Since the force control of flexible manipulators with planar one or two links using the distributed-parameter modeling has been the subject of a considerable number of publications until now, real time computations of the force control schemes are possible. But, application of those control schemes to multi-link spatial manipulators is fairly complicated. In this paper, we apply a concise hybrid position/force control scheme for a flexible manipulators. We use a lumped-parameter modeling for the flexible manipulators. The Hamilton's principle is applied to derive the equations of motion for the system and then, state-space model is obtained by the Lagrange's method. Finally, comparison of simulation results with experimental results is given to show the performance of our method.

Keywords Hybrid position/force control, Flexible manipulator, Lumped-parameter model, State-space model, Simulation.

1 Introduction

The research on force control of rigid manipulators began as early as 1960's but, the algorithm was systemized over 1970's to 1980's. The approaches developed are widely divided into hybrid position/force control schemes and impedance control schemes [1)2)]. So, until now, force control has been one of the hottest research topics. However, force control of flexible manipulators just began in 1985 by Fukuda [3)].

Chiou and Shahinpoor have pointed out that the link flexibility is one of the causes of dynamic instability. They have extended their research from planar one link flexible manipulator to two link manipulator, analyzing their stability by applying hybrid position/force control schemes [4)].

Matsuno *et al* have addressed the quasi-static hybrid position/force control scheme and dynamic hybrid position/force control scheme for the planar two DOF manipulator with flexible second link [5)].

Kojima and Kawanabe have constructed the PIS control scheme which makes good use of the flexibilty of robot. In this scheme, without using a force sensor, the feedback of strain gauge has been used to control the contact force [6)].

For force control of flexible manipulators, inverse kinematic task is an essence, and has been proposed by Svinin and Uchiyama [7)].

In some multi-link spatial flexible manipulators, equations of motion depend upon arm's configuration, and thus, simple models are required for real time computation, so lumped-parameter models are effective for such purpose [8)]. However, so far, there has been no formulation of equations of motion for force control by the lumped-parameter modeling.

In this paper, a simple simulation model for flexible manipulator under constraints is constructed by lumped-parameter method, and the equations of motion are obtained by applying Hamilton's principle. The state-space model is obtained by Lagrange's method and analyzed on MATLAB. In the second step, a precise simulation model is developed using ADAMS™, which is a general purpose 3-dimensional analysis software.

In order to simplify the discussions, we take the case of a 2-link manipualtor moving in vertical plane only, and apply concise hybrid position/force control scheme. Finally, the experiments and simulations are performed, comparison of simulation results with experimental results is given to show the performance of our method.

2 Modeling of constrained flexible manipulator

2.1 Constraint equation

The constraints are divided into time-independent scleronomous , and time-dependent rheonomous contrains [9)]. In this paper, only rheonomous contraints are considered which can be written in the following form

$$\varphi(q,t) = 0, \tag{1}$$

where $\varphi \in \Re^l$.

2.2 Equations of motion

By using lumped-paramater model of the flexible manipulators, equations of motion can be derived by using the Hamilton's principle, and can be written as

$$\begin{bmatrix} \tau \\ 0 \end{bmatrix} = \begin{bmatrix} M_{11}(q) & M_{12}(q) \\ M_{21}(q) & M_{22}(q) \end{bmatrix} \begin{bmatrix} \ddot{\theta} \\ \ddot{e} \end{bmatrix} + \begin{bmatrix} h_1(q,\dot{q}) \\ h_2(q,\dot{q}) \end{bmatrix} + \begin{bmatrix} 0 & 0 \\ 0 & K_{22} \end{bmatrix} \begin{bmatrix} \theta \\ e \end{bmatrix} + \begin{bmatrix} g_1(q) \\ g_2(q) \end{bmatrix} + \begin{bmatrix} J_{\varphi\theta}^T\lambda \\ J_{\varphi e}^T\lambda \end{bmatrix}, \tag{2}$$

or in a compact form

$$L\tau = M(q)\ddot{q} + h(q,\dot{q}) + Kq + g(q) + J_\varphi^T\lambda, \tag{3}$$

where

$q = \begin{bmatrix} \theta \\ e \end{bmatrix}$: coordinate vectors,

$\theta \in \Re^n$ are the joint rotations,

$e \in \Re^m$ are the the elastic deflections,

τ : joint torque vector ($\Re^n$),

$M(q)$: inertia matrix,

$h(q, \dot{q})$: vector of centrifugal and Coriolis forces,

$g(q)$: vector of gravity,

J_φ : Jacobian matrix for constraints ($\Re^{(n+m)\times l}$),

λ : vector of Lagrange mutiplier ($\Re^l$), and

L : tranformation matrix,

$L = \begin{bmatrix} I^T_{n\times n} & 0^T_{m\times n} \end{bmatrix}^T.$

J. G. Jalón and E. Bayo have used the same constraint Jacobian matrix for both rheonomously and scleronomously constrained systems [9]. Therefore, here we can use Jacobian matrix for rheonomous constraints as

$$\begin{aligned} J_\varphi &= \frac{\partial\varphi}{\partial p} J_q(q) \\ &= \begin{bmatrix} \frac{\partial\varphi}{\partial\theta_1} & \frac{\partial\varphi}{\partial\theta_2} & \cdots \frac{\partial\varphi}{\partial\theta_n} & \frac{\partial\varphi}{\partial e_1} & \frac{\partial\varphi}{\partial e_2} & \cdots \frac{\partial\varphi}{\partial e_m} \end{bmatrix} \\ &= \begin{bmatrix} J_{\varphi\theta} & J_{\varphi e} \end{bmatrix}, \end{aligned} \tag{4}$$

where $J_q = [J_\theta \; J_e]$ is standard Jacobian matrix of the manipulator, and p represents the cartesian coordinates of the end-effector's origin and the three euler angles. Lagrange mutiplier can be presented as

$$\lambda = \frac{f_n}{|\mathrm{grad}\varphi|}, \quad \mathrm{grad}\varphi = \frac{\partial\varphi}{\partial p}, \tag{5}$$

where f_n is the component of contact force normal to the constraints, gradφ is the gradient of constraint equations φ (from now onward, gradφ is expressed by $\nabla\varphi$).
In order to simplify Eqs. (2) and (3), we make the following assumptions

- Only the slow motion is considered, and thus the centrifugal and Corioli's forces can be neglected,

$$h(q, \dot{q}) = 0,$$

- The influence of elastic deflection e is supposed to be small, and thus,

$$M(\theta, e) \approx M(\theta), \quad g(\theta, e) \approx g(\theta).$$

In the stationary condition (i.e., $\ddot{\theta} = \dot{\theta} = 0$ and $\ddot{e} = \dot{e} = 0$), Eq. (2) becomes

$$\begin{bmatrix} \tau_0 \\ 0 \end{bmatrix} = \begin{bmatrix} 0 & 0 \\ 0 & K_{22} \end{bmatrix} \begin{bmatrix} \theta_0 \\ e_0 \end{bmatrix} + \begin{bmatrix} g_1(\theta_0) \\ g_2(\theta_0) \end{bmatrix} + \begin{bmatrix} J^T_{\varphi\theta}\lambda_0 \\ J^T_{\varphi e}\lambda_0 \end{bmatrix}, \tag{6}$$

where τ_0 is the static torque to keep arm in the configuration to balance the gravity and contact force, e_0 is the static deflection for the links in the configuration due to gravity and contact force, and θ_0, λ_0 are respectively the angle and the Lagrange multiplier for the static condition. In addition, Δe , $\Delta\tau$, $\Delta\theta$ and $\Delta\lambda$ can be respectively expressed as follows

$$\begin{aligned} \Delta\tau &= \tau - \tau_0 = \tau - (g_1(\theta_0) + J^T_{\varphi\theta}\lambda_0), \\ \Delta e &= e - e_0 = e + K^{-1}_{22}(g_2(\theta_0) + J^T_{\varphi e}\lambda_0), \\ \Delta\theta &= \theta - \theta_0, \\ \Delta\lambda &= \lambda - \lambda_0. \end{aligned} \tag{7}$$

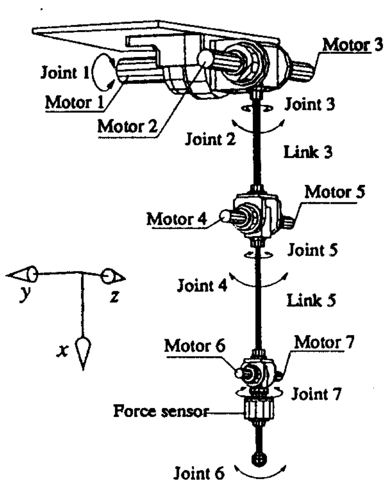

Fig. 1 Experimental robot with 2 links and 7 joints.

Incorporating Eq. (7) along with above assumptions into Eq. (2) can be written in a compact form as

$$L\Delta\tau = M(\theta)\Delta\ddot{q} + K\Delta q, + J^T_\varphi\Delta\lambda, \tag{8}$$

where $\Delta q = [\ \Delta\theta^T \quad \Delta e^T\ ]^T$.
The environment is modeled as a spring with a large spring constant. the Lagrange mutiplier $\Delta\lambda$ is given by

$$\Delta\lambda = K_{env} n^T \Delta p = K_{env} n^T (J_\theta \Delta\theta + J_e \Delta e), \tag{9}$$

where K_{env} is the environmental stiffness, Δp is the deflection of the constraints and $n = \frac{\nabla\varphi}{|\nabla\varphi|}$ is a unit normal vector of the constraints. Substituting Eq. (9) into Eq. (8), the approximated equations of motion can be written as

$$\begin{bmatrix} \Delta\tau \\ 0 \end{bmatrix} = \begin{bmatrix} M_{11}(\theta) & M_{12}(\theta) \\ M_{21}(\theta) & M_{22}(\theta) \end{bmatrix} \begin{bmatrix} \Delta\ddot{\theta} \\ \Delta\ddot{e} \end{bmatrix} + \begin{bmatrix} J_{\varphi\theta} K_{env} n J_\theta & J_{\varphi\theta} K_{env} n J_e \\ J_{\varphi e} K_{env} n J_\theta & K_{22} + J_{\varphi e} K_{env} n J_e \end{bmatrix} \begin{bmatrix} \Delta\theta \\ \Delta e \end{bmatrix}, \tag{10}$$

or in a more compact form

$$L\Delta\tau = M(\theta)\Delta\ddot{q} + K^*\Delta q, \tag{11}$$

3 Simulations and Experiment

To clarify the discussion, the motions of an experimental flexible manipulator called ADAM having 2 elastic links and 7 rotary joints (Fig. 1) are considered. The discussion is restricted to only the vertical motion of joint angles 2, 4 and 6 (θ_2, θ_4, θ_6) while joint angle 6 always preserves $\pi/2$ [rad] with respect to constraints.
Based on above model, two simulations are performed. The results, achieved by a precise model constructed by commercial dynamic analysis software packages, are compared with experimental results.

3.1 Experimental setup

The experimental manipualtor ADAM is driven by DC servo motors with hardware velocity feedback servo. Each of motors 1-3 has an optical encoder for sensing the joint angle and a tachometer for sensing the joint

Table 1 ADAM link parameters.

	Link 3	Link 5
Length	0.5 m	0.5 m
Elastic part	0.359 m	0.394 m
Diameter	0.013 m	0.01 m
Material	SUP-6	SUP-6
EI	288.1 Nm^2	100.8 Nm^2
Mass	0.7 kg	0.5 kg

angular velocity. None of the motors 4-7 has a tachometer, and thus, pulse signals generated by optical encoder are translated into velocity signals through F/V (Frequency to Voltage) converter.
The parameters of each link of ADAM are presented in Table 1. Strain gauges are used to measure the link vibration while a laser beam and a force sensor is used to measure the contact force at end-effector.

3.2 Control scheme

As ADAM is equipped with the velocity feedback servo motors, so joint motion is commanded by joint velocity command, and therefore joint torque cannot be controlled directly. Hence, we assume the relationship between velocity command and the produced torque as follows:

$$\begin{aligned} \tau &= G_r K_{sp}(V_{ref} - K_{sv}\dot{\theta}_m), \\ &= \Lambda(\dot{\theta}_c - \dot{\theta}), \end{aligned} \quad (12)$$

where

G_r	:	gear reduction ratio,
K_{sp}	:	voltage feedback gain,
K_{sv}	:	voltage/velocity coefficient,
$\dot{\theta}_m = G_r\dot{\theta}$	:	angular velocity of motor,
V_{ref}	:	voltage velocity command,
$\dot{\theta}_c$	:	velocity command, and
$\Lambda = G_r{}^2 K_{sp} K_{sv}$	:	velocity feedback gain.

Voltage velocity command V_{ref} is computed by

$$V_{ref} = G_r K_{sv}\dot{\theta}_c, \quad (13)$$

and is used in the experiments.
As we can see, from Eq. (6), that the elastic deflection is dependent upon the contact force when the manipulator moves slowly enough. So the vibration of manipulator can be suppressed by controlling the contact force. The approximate joint velocities $\dot{\theta}_c$ can be computed as follows

$$\dot{\theta}_c = \dot{\theta}_t + \dot{\theta}_f, \quad (14)$$

where $\dot{\theta}_t$ is the approximate joint velocity for positioning while $\dot{\theta}_f$ is additional factor for force control. The vlocities $\dot{\theta}_t$ and $\dot{\theta}_f$ are respectively computed as

$$\begin{aligned} \dot{\theta}_t &= J_\theta^T(I - \nabla\varphi^T\nabla\varphi)K_{tp}(p_d - p), \\ \dot{\theta}_f &= \Lambda^{-1}J_\theta^T\nabla\varphi^T K_{fp}(\lambda_d - \lambda), \end{aligned} \quad (15)$$

where I is unit matrix. $\nabla\varphi$, $(I - \nabla\varphi^T\nabla\varphi)$ define matrties which respectively select force and position directions. K_{tp} is position gain matrix for positioning while K_{fp} is for force control.

From Eq. (7) we have

$$\Delta\tau = \Lambda\{(\dot{\theta}_c - \dot{\theta}) - \Lambda^{-1}(g_1(\theta_0) + J_{\varphi\theta}^T\lambda_0)\}. \quad (16)$$

If the velocity servo loop is sufficiently stiff, that is , the gains Λ are high, the term $\Lambda^{-1}(g_1(\theta_0) + J_{\varphi\theta}^T\lambda_0)$ can be neglected. For stationary condition, $\theta_0 \approx 0$, Eq. (16) becomes

$$\Delta\tau = \Lambda\{(\dot{\theta}_c - \dot{\theta}_0) - \{(\dot{\theta} - \dot{\theta}_0)\} = \Lambda(\Delta\dot{\theta}_c - \Delta\dot{\theta}). \quad (17)$$

Then, substituting Eq. (16) into Eq. (11) and taking into account the fact that $\Delta\dot{\theta} = L^t\Delta\dot{q}$, the equations of motion of constrained flexible manipulator are obtained as

$$M\Delta\ddot{q} + L\Lambda L^T\Delta\dot{q} + K^*\Delta q = L\Lambda\Delta\dot{\theta}_c. \quad (18)$$

Eq. (18) can be transformed into the state space form as

$$\begin{bmatrix} \Delta\ddot{q} \\ \Delta\dot{q} \end{bmatrix} = \begin{bmatrix} -M^{-1}L\Lambda L^T & -M^{-1}K^* \\ I & 0 \end{bmatrix} \times \begin{bmatrix} \Delta\dot{q} \\ \Delta q \end{bmatrix} + \begin{bmatrix} M^{-1}L\Lambda \\ 0 \end{bmatrix}\Delta\dot{\theta}_c, \quad (19)$$

Eq. (19) can be cast into state space equation form as follows:

$$\Delta\dot{x} = A\Delta x + B\Delta\dot{\theta}_c. \quad (20)$$

In the simulations, the discrete-time state equation corresponding to Eq. (20) is used in the following form:

$$\Delta x(k+1) = \Phi\Delta x(k) + \Gamma\Delta\dot{\theta}_c(k), \quad (21)$$

where k indicates the k-th interval of the sampling process, Φ and Γ are the discrete matrices of A and B for a zero-order holder (ZOH).

3.3 A precise model

A precise model of ADAM is constructed by ADAMS™. ADAMS™ is a commercial software package for dynamic analysis of mechanical systems produced by Mechanical Dynamics, Inc. In this simulator, a finite-element method based on Timosenko beam theory is used as a modeling method of flexible structures. In order to obtain a precise model, the elastic beam is divided into five pieces.

3.4 Results and Discussion

We present the experimental and simulations results for the case when end-effector is not moving, and When it is moving. The constaint is a vertical plane located at 0.375m in the y direction from the robot's reference coordinates.
The responses of task motion and contact force at the tip, as achieved by simulations and experiments, are shown in **Fig. 2** and **Fig. 3** respectively.
In **Fig. 2**, K_{tp} = diag[1 1] [rad/(m·s)] and K_{fp} = 0.2 [rad/(N·s)], and in **Fig. 3**, K_{tp} = diag[4 4] [rad/m·s] and K_{fp} = 0.4 [rad/(N·s)].
The sampling time is set as 10 (ms), and for these simulations, K_{sp} [Nm/V] of Eq. (12) is decided to be approximated to the experimental results, and the environmental stiffness is taken as 5000 [N/m].

Fig. 2 and **Fig. 3** point out that our control scheme is effective for flexible manipulator modelled by lumped-paramater modeling method.
In case of slow motion of manipulator, contact force is controlled without suppressing vibration because of dependency between elastic deflection of link and contact force.

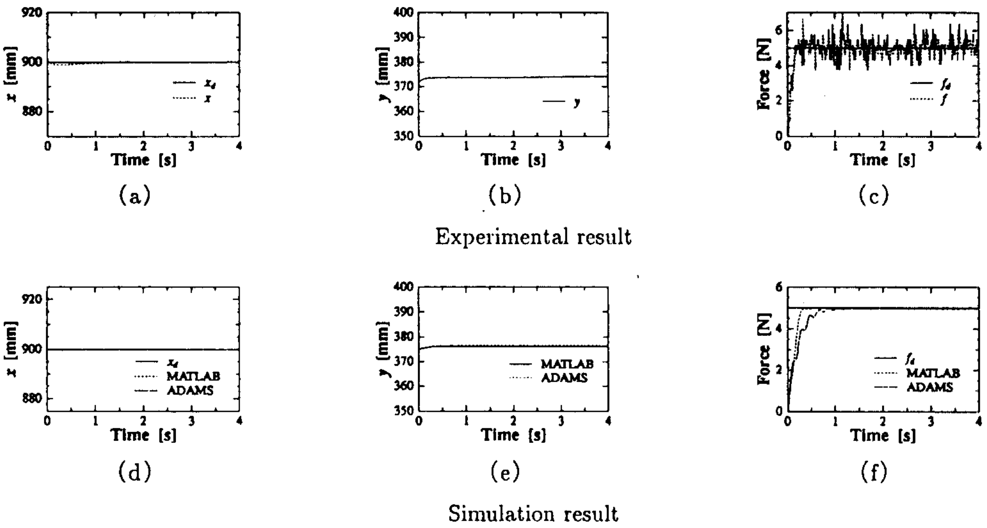

Fig. 2 When end-effector of robot arm does not move.

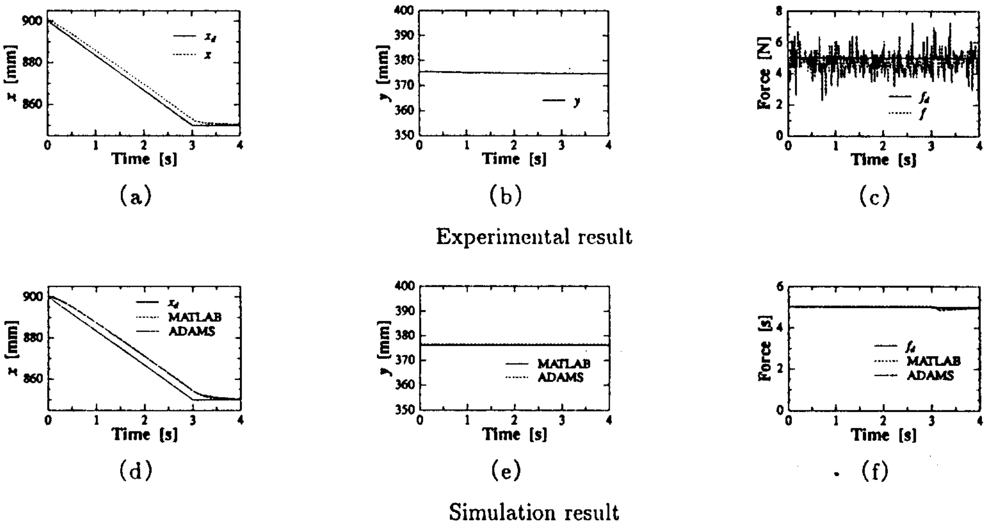

Fig. 3 When end-effector of robot arm moves.

4 Conclusions

A hybrid position/force control shemes for flexible manipulators has been discussed. Exprimental results show that the system responses are in good agreement with simulation results. Investigating these results, it can be concluded that our control scheme is effective.

References

1) M. H. Raibert and J. J. Craig, "Hybrid position/force control of manipulators," Trans. ASME, J. of Dynamic System, Measurement and Control, vol. 103, no. 2, pp. 126–133, 1981.

2) M. T. Mason, "Compliance and force control for computer controlled manipulators," IEEE Trans. on Systems, Man and Cybernetics, vol. SMC-11, pp. 418–432 1981.

3) T. Fukuda, "Flexibility control of elastic robotic arms," J. Robotic Systems, vol. 2, no. 1, pp. 73–88, 1985.

4) B. C. Chiou and M. Shahinpoor, "Dynamics Stability Analysis of a One-Link Force-Controlled Flexible Manipulator," J. Robotic Systems, vol. 5, no. 5, pp. 443–451, 1988.

5) F. Matsuno and K. Yamammoto, "Dynamic Hybrid Position/Force Contorl of a Flexible Manipulator," Proc. of the IEEE Int. Conf. on Robotics and Automation, vol. 2, pp. 462–467, 1993.

6) H. Kojima and T. Kawanabe, "Position and Force Control of Flexible Robot Arm with PIS Control," J. Robotics Society of Japan, vol. 10, no. 3, pp. 353–360, 1992.

7) M. M. Svinin and M. Uchiyama, "Contribution to Inverse Kinematics of Flexible Robot Arm," Int. J. JSME, Series C, vol. 37, no. 4, pp. 755–764, 1994.

8) A. Konno and M. Uchiyama, "Modeling of a Flexible Manipulator Dynamics Based on the Holzer's Method," J. of Robotics Society of Japan, vol. 12, no. 7,pp. 1021–1028, 1991 (in Japanese).

9) J. G. Jalón and E. Bayo, Kinematic and Dynamic Simulation of Multibody System, Springer-Verlag New York, 1994.